Crucial function of vertebrate glutaredoxin 3 (PICOT) in iron homeostasis and hemoglobin maturation

Petra Haunhorst[a],*, Eva-Maria Hanschmann[a,b],*, Lars Bräutigam[c], Oliver Stehling[a], Bastian Hoffmann[a], Ulrich Mühlenhoff[a], Roland Lill[a,d], Carsten Berndt[c,e], and Christopher Horst Lillig[a,b]

[a]Institute for Clinical Cytobiology and Cytopathology, Faculty of Medicine, Philipps-Universität, 35037 Marburg, Germany; [b]Institute for Medical Biochemistry and Molecular Biology, University Medicine, Ernst-Moritz Arndt University, 17489 Greifswald, Germany; [c]Division of Biochemistry, Department for Medical Biochemistry and Biophysics, Karolinska Institutet, 171 77 Stockholm, Sweden; [d]Max-Planck-Institut für Terrestrische Mikrobiologie, 35043 Marburg, Germany; [e]Department of Neurology, Medical Faculty, Heinrich-Heine Universität, 40225 Düsseldorf, Germany

ABSTRACT The mechanisms by which eukaryotic cells handle and distribute the essential micronutrient iron within the cytosol and other cellular compartments are only beginning to emerge. The yeast monothiol multidomain glutaredoxins (Grx) 3 and 4 are essential for both transcriptional iron regulation and intracellular iron distribution. Despite the fact that the mechanisms of iron metabolism differ drastically in fungi and higher eukaryotes, the glutaredoxins are conserved, yet their precise function in vertebrates has remained elusive. Here we demonstrate a crucial role of the vertebrate-specific monothiol multidomain Grx3 (PICOT) in cellular iron homeostasis. During zebrafish embryonic development, depletion of Grx3 severely impairs the maturation of hemoglobin, the major iron-consuming process. Silencing of human Grx3 expression in HeLa cells decreases the activities of several cytosolic Fe/S proteins, for example, iron-regulatory protein 1, a major component of posttranscriptional iron regulation. As a consequence, Grx3-depleted cells show decreased levels of ferritin and increased levels of transferrin receptor, features characteristic of cellular iron starvation. Apparently, Grx3-deficient cells are unable to efficiently use iron, despite unimpaired cellular iron uptake. These data suggest an evolutionarily conserved role of cytosolic monothiol multidomain glutaredoxins in cellular iron metabolism pathways, including the biogenesis of Fe/S proteins and hemoglobin maturation.

INTRODUCTION

Iron is an essential trace element for most organisms. In the form of heme or iron–sulfur (Fe/S) cofactors, it facilitates the transport of oxygen or electrons, serving important functions in respiration, citric acid cycle, lipid metabolism, gene regulation, and DNA synthesis and repair (Cairo *et al.*, 2006). Iron acquisition, transport, and storage need to be tightly regulated to prevent both iron deficiency and toxic iron overload. In vertebrates, uptake, intracellular distribution, and storage of iron are regulated mainly posttranscriptionally by the iron-regulatory proteins (IRPs) IRP1 and IRP2 (Muckenthaler *et al.*, 2008; Hentze *et al.*, 2010). Under iron limitation, both proteins bind to iron-responsive elements (IREs) on mRNAs encoding proteins involved in iron metabolism. Under iron sufficiency, IRP1 binds an Fe/S cluster and acts as a cytosolic aconitase. IRP2 does not

coordinate a Fe/S center and is instead regulated by FBXL5-mediated proteasomal degradation (Guo et al., 1995; Salahudeen et al., 2009; Vashisht et al., 2009). The major iron-consuming process in vertebrates is erythropoiesis. Two to three million erythrocytes are produced every second, consuming 30 mg of iron for heme production per day in humans (Li and Ginzburg, 2010). Heme is generated by various biosynthetic steps in mitochondria and the cytosol. The mRNA of the erythrocyte-specific isoform of mitochondrial δ-aminolevulinic acid synthase (eALAS), the rate-limiting enzyme in heme synthesis, contains an IRE in its 5′-untranslated region and is efficiently translated only when iron is available. In iron deficiency, protoporphyrin synthesis is down-regulated by apo-IRP1 and apo-IRP2 binding to the IRE of the eALAS mRNA (Schranzhofer et al., 2006).

The passage of iron through the cytosol, from a "labile iron pool" to iron-dependent proteins within different compartments, has long been an open question (Richardson and Ponka, 1997; Shi et al., 2008). Only recently have the first proteins involved in this process been identified. The mammalian poly(rC)-binding proteins 1 and 2 (PCBP1 and PCBP2) act as cytosolic iron chaperones for efficient insertion of iron into ferritin and the hypoxia-inducible factor prolyl hydroxylase (Shi et al., 2008; Nandal et al., 2011). The cytosolic monothiol glutaredoxins 3 and 4 (Grx3/Grx4) are key players of fungal iron metabolism. Their depletion in Saccharomyces cerevisiae specifically impairs iron-requiring reactions in the cytosol, mitochondria, and nucleus, including the synthesis of Fe/S clusters, heme, and di-iron centers, suggesting a central role of Grx3/Grx4 in the delivery of iron within the cytosol and to other compartments (Mühlenhoff et al., 2010). In addition, these proteins are involved in iron uptake regulation in yeast and other fungi by interacting with iron-responsive transcription factors (Ojeda et al., 2006; Herrero and de la Torre-Ruiz, 2007; Jbel et al., 2011). Generally, dithiol (active-site motif Cys-Pro-Tyr-Cys) and monothiol (Cys-Gly-Phe-Ser) Grxs have been classified (Lillig et al., 2008). Dithiol Grxs reduce protein disulfides and glutathione-mixed disulfides, thus regulating protein function and various cellular pathways. The function of monothiol Grxs is much less understood, especially considering that most members do not undergo redox chemistry (Herrero and de la Torre-Ruiz, 2007; Lillig et al., 2008). Some dithiol and most monothiol Grxs bind a [2Fe-2S] cluster that is coordinated by two protein monomers and two glutathione molecules (Lillig et al., 2005; Feng et al., 2006; Picciocchi et al., 2007). Monothiol Grxs lacking additional domains (i.e., single-domain monothiol Grxs) are conserved from bacteria to human. In nonphotosynthetic eukaryotes, these proteins are located in mitochondria and termed Grx5. Yeast mutants lacking Grx5 exhibit a severely deregulated cellular iron homeostasis and show defects in the maturation of Fe/S proteins (Rodríguez-Manzaneque et al., 1999, 2002; Mühlenhoff et al., 2003). Deficiency of Grx5 in zebrafish and humans results in impaired biosynthesis of Fe/S clusters and heme (Wingert et al., 2005; Camaschella et al., 2007). The second class of monothiol Grxs, multidomain monothiol Grxs, is restricted to eukaryotes. These proteins consist of one Trx domain followed by one to three Grx domains. Yeast Grx3 and Grx4 contain one Grx domain each, whereas their vertebrate homologues possess two Grx domains. Human Grx3 (also named PICOT, TXNL-2, and HUSSY-22) has been implicated in various signaling pathways that lead to the activation of cells. Originally identified as an interaction partner of protein kinase C-θ, Grx3 was reported to function, for instance, in the activation of T-cells through inhibition of mitogen-activated kinase and nuclear factor-κB signaling (Witte et al., 2000), the attenuation of cardiac hypertrophy by inhibiting calcineurin-nuclear factor of activated T-cell signaling (Jeong et al., 2006, 2008), and p53-dependent neuronal differentiation (Brynczka et al., 2007). The molecular function of Grx3 in these regulatory processes, however, is unclear.

Here we examine the potential role of Grx3 from higher eukaryotes in iron homeostasis, which mechanistically differs in many aspects from that of fungi. As a first model organism we used zebrafish and examined the role of Grx3 in hematopoiesis. Second, Grx3 was depleted in human cell culture to study the effects on various aspects of iron homeostasis such as heme biosynthesis, Fe/S protein biogenesis, and cellular iron uptake. Collectively, our results support a central role of vertebrate Grx3 in cellular iron homeostasis, closely resembling physiological functions of yeast Grx3/Grx4.

RESULTS

Zebrafish Grx3 is required for hemoglobin maturation

The genome of the zebrafish (zf) Danio rerio encodes a Grx3-related protein (zfGrx3; gene name glrx3) that is 59% identical to human Grx3 and 37% identical to yeast Grx3 and Grx4. Similar to mammalian Grx3, zfGrx3 contains an N-terminal Trx and two monothiol Grx domains (Supplemental Figure S1). In situ hybridization revealed the presence of zfGrx3 transcripts in eye, brain, heart, and a ventral region that most likely constitutes the intermediate cell mass, the site of embryonic erythropoiesis (Figure 1A).

To address potential functions of zfGrx3 in vivo, we injected a morpholino targeted against the translation initiation site of zfGrx3 into one-cell-stage embryos. Morpholino injection reduced the levels of Grx3 protein in a pool of ~250 embryos to 40% (Figure 1B) compared with the levels of the protein in control embryos. Grx3 knockdown did not induce gross morphological changes (Supplemental Figure S2). However, in contrast to wild-type embryos, fewer red blood cells were visible in the heart of embryos lacking Grx3. The effect of zfGrx3 depletion on hemoglobin maturation and iron metabolism was investigated in more detail by visualization of hemoglobin at 48 h postfertilization (hpf) using diaminofluorene (DAF; Figure 1, C and D) and o-dianisidine (Figure 1, F and G) staining. In summary, 90% (n = 191) of wild-type embryos showed clear hemoglobin staining. This amount decreased to 38% (n = 275) in zfGrx3-knockdown embryos. The specificity of this phenotype for the loss of Grx3 was demonstrated by simultaneous injection of 40 pg of zfGrx3 capped mRNA together with the morpholino, which restored the amount of positively stained embryos to 84% (n = 45; Figure 1E). To verify that the loss of Grx3 function specifically affected heme synthesis and not erythropoiesis in general, we analyzed the expression of β-globin by in situ hybridization (Figure 1, F and G). In contrast to heme, the expression of β-globin transcripts was not dependent on the presence of Grx3 (100% positives in n = 37 embryos). Thus depletion of zfGrx3 specifically impaired the synthesis of heme.

The inability of Grx3-depleted fish to synthesize heme could be the result of an impaired Fe/S cluster maturation of IRP1, leading to an augmented binding to the 5′-IRE of eALAS, the first enzyme of heme synthesis in erythrocytes. This would lead to a translational repression of eALAS in erythropoietic tissues, as observed upon depletion of the mitochondrial Fe/S cluster biogenesis protein Grx5 (Wingert et al., 2005). In fact, the loss of Grx3 function led to a significant reduction in ALAS2 levels in the fish (Figure 2A). The repression of eALAS could be overcome by abrogation of the expression of IRP1 in Grx5-depleted fish (Wingert et al., 2005). We tested this possibility for Grx3 depletion. Unlike in the case of Grx5-depleted fish, however, the Grx3-IRP1 double knockdown did not rescue but instead exacerbated the anemic phenotype of embryos lacking zfGrx3. The number of embryos containing wild-type level
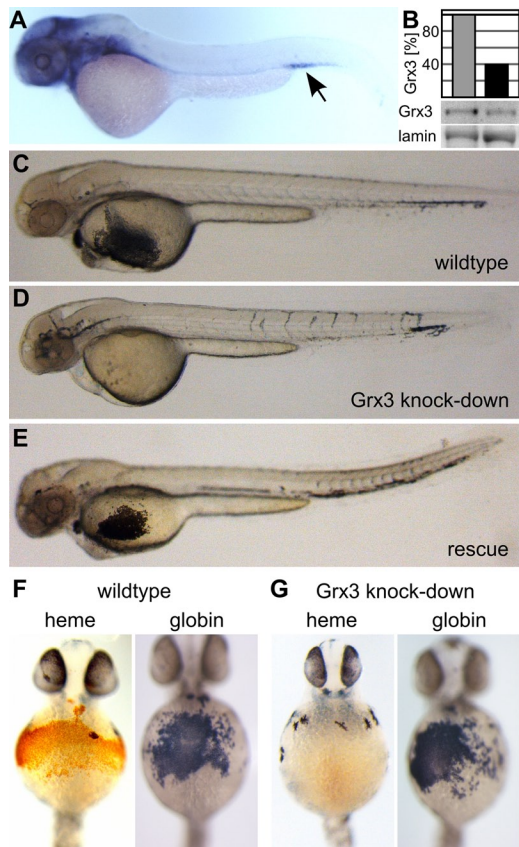
FIGURE 1: Depletion of Grx3 in zebrafish embryos causes loss of hemoglobin. (A) In situ hybridization of a zebrafish embryo at 48 hpf with a zfGrx3-specific DNA probe. The arrow indicates the region most likely constituting the intermediate cell mass, the site of embryonic erythropoiesis. (B) Western blot quantification of Grx3, relative to the loading control lamin, from wild-type and a pool of ~250 morpholino-injected embryos. (C–G) Positive hemoglobin staining of zebrafish embryos at 48 hpf depends on the presence of zfGrx3. Diaminofluorene staining of (C) wild-type embryos, (D) zfGrx3-knockdown embryos, and (E) embryos injected with both morpholino and capped mRNA coding for zfGrx3. (F–G) o-Dianisidine staining and β-globin–specific in situ hybridization of (F) wild-type and (G) zfGrx3-knockdown embryos. One typical embryo is shown to exemplify each phenotype.

of hemoglobin (Figure 2, B and F) dropped to 10% ($n = 40$; Figure 2C), compared with 38% for zfGrx3 depletion (see earlier discussion). Of note, IRP1 silencing itself substantially impaired hemoglobin maturation, and only 18% of IRP1-depleted embryos displayed the normal hemoglobin phenotype ($n = 95$; Figure 2, D and F), possibly as a result of impaired iron uptake. Strikingly, this loss could be rescued to 87% ($n = 40$) of wild-type levels by simultaneous overexpression of zfGrx3 (Figure 2, E and F). These findings suggest that the zfGrx3 function in iron metabolism is independent of the regulatory role of IRP1 and that zfGrx3 overexpression can overcome the defects in iron homeostasis upon IRP1 depletion, possibly by improving iron utilization under these low-iron conditions. In other words, overproduction of zfGrx3 overrides the regulatory function of IRP1.

Next we biochemically analyzed the maturation efficiency of iron-dependent proteins upon loss of zfGrx3 function. We first measured the enzyme activity of the Fe/S protein aconitase in total cell extracts of zfGrx3-knockdown and wild-type embryos at 48 hpf. In

zfGrx3-depleted extracts the total aconitase activity, that is, the sum of the cytosolic and mitochondrial isoforms, was reduced significantly to 79% compared with controls (Figure 3A). As a second iron-dependent protein, we analyzed the activity of mitochondrial cytochrome *c* oxidase (COX), an enzyme relying on heme a/a$_3$. Similar to aconitase activity, zfGrx3 morpholino–injected embryos contained only 82% COX activity relative to controls (Figure 3B). In contrast, the activity of malate dehydrogenase as an iron-independent enzyme did not change (Figure 3C). Given the amount of reduction in Grx3 in the pooled embryos to 40% (Figure 1B), the small but consistent drop of iron-dependent enzyme activities by 20% indicates that zfGrx3 is important for the maturation of these two iron-dependent enzymes. Together these results suggest a crucial role for zfGrx3 in iron metabolism in the erythropoietic cell lineage and likely also in other tissues.

Depletion of human Grx3 specifically affects cytosolic iron metabolism

To investigate the potential role of vertebrate Grx3 in cellular iron homeostasis in more detail, we depleted human Grx3 in HeLa cell cultures by short interfering RNA (siRNA) and studied the consequences for cellular iron metabolism. Cells transfected with unspecific scrambled siRNA served as a control. After two consecutive rounds of transfection with Grx3-specific siRNAs followed by 3–4 d of cell growth, that is, 6–7 d after the first transfection, the mRNA levels of Grx3 were <2% of control cells as determined by quantitative real-time PCR. About 10 ± 2% residual Grx3 protein could be detected in Western blots (Figure 4, A and B).

First, we studied the effect of Grx3 depletion on the steady-state levels and activities of two cytosolic Fe/S proteins: IRP1 and glutamine phosphoribosyl-pyrophosphate amidotransferase (GPAT). IRP1 protein levels were estimated by Western blotting and found to be decreased more than twofold upon Grx3 depletion, an effect typical for defects in the maturation of this Fe/S protein (Figure 4, A and B). We therefore quantified the aconitase activity of IRP1 using cytosolic fractions obtained from the cells; the efficiency of the cell fractionation procedure is documented in Supplemental Figure S4. Compared to control cells, the activity of cytosolic aconitase in Grx3-depleted cells decreased to 40% (Figure 4C). Similar results were obtained for GPAT, which is translated within the cytosol as an inactive proenzyme (Zhou *et al.*, 1992). Maturation to the active enzyme requires both the incorporation of a [4Fe-4S] cluster and the subsequent removal of an 11–amino acid residue–long propeptide at the N-terminus. Failure to insert the Fe/S cluster results in degradation of the precursor, and thus the levels of GPAT are a reliable measure of Fe/S cluster assembly. On depletion of Grx3 in HeLa cells, the steady-state levels of GPAT decreased twofold relative to controls, indicating insufficient Fe/S cluster insertion (Figure 4, A and B).

Essentially identical effects on IRP1 and GPAT were seen upon Grx3 knockdown with different sets of Grx3-specific siRNAs, confirming the specificity of the siRNA procedure and the cellular implications (Supplemental Figure S3). These results demonstrate that the maturation of cytosolic Fe/S proteins crucially depends on Grx3 function.

The severe affect of Grx3 depletion on the aconitase activity of cytosolic IRP1 suggested an increase in the apo relative to the holo form of this protein and, consequently, effects on the regulation of the iron metabolism. To assay for such changes, we analyzed the ability of IRP1 to bind to the [γ-^{32}P]CTP-labeled IRE of ferritin mRNA by using a RNA electrophoretic mobility shift assay. The IRE-binding activity of IRP1 was measured independently from that of IRP2 by
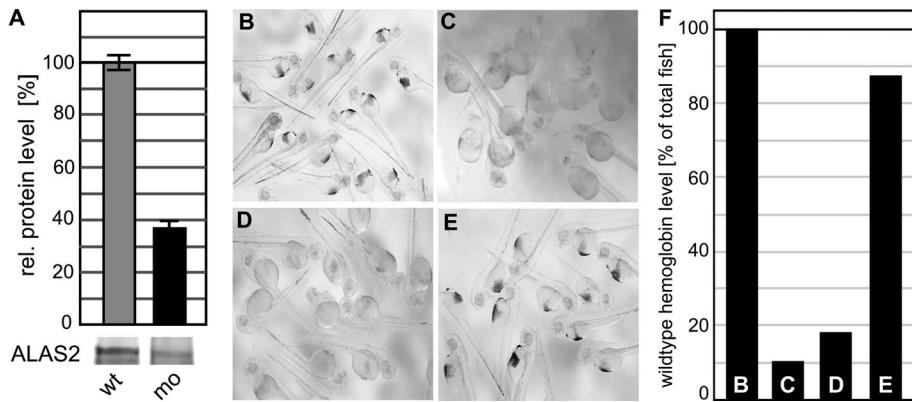
FIGURE 2: Zebrafish Grx3 function in iron homeostasis is independent of IRP1. (A) Detection of ALAS2 levels in wild-type embryos and embryos depleted for Grx3. Diaminofluorene staining of hemoglobin at 48 hpf in (B) wild-type embryos ($n = 30$), (C) embryos depleted for IRP1 ($n = 95$), (D) embryos depleted for both IRP1 and zfGrx3 ($n = 40$), and (E) embryos depleted for IRP1 and overexpressing zfGrx3 by injection of zfGrx3 mRNA ($n = 39$). Knockdown of IRP1 and zfGrx3 was induced by injection of specific morpholinos into single-cell eggs. (F) Quantification of the experiments in B–E relative to wild-type fish.

inducing an antibody-mediated supershift on IRP2 (Stehling *et al.*, 2008). The decreased IRP1 protein levels in Grx3-deficient cells (Figure 4, A and B) were taken into account by following the maximal IRE-binding capacity of IRP1 after treatment of samples with β-mercaptoethanol (β-ME). The ratio of IRP1 binding in the absence and presence of β-ME thus reflects the IRE-binding capacity of IRP1. This value increased almost twofold in cells depleted for Grx3 relative to cells treated with scrambled siRNAs (Figure 4D, middle, and Supplemental Figure S5B). In contrast, both the levels and the IRE-binding activity of IRP2 were only mildly affected (Figure 4, A and D, right, and Supplemental Figure S5C). Overall, a 1.5-fold increase of

IRE binding capacity was observed, suggesting a cytosolic iron starvation condition in the absence of Grx3 (Figure 4D, left). To directly test this, we analyzed the consequences of IRP1 activation for the levels of transferrin receptor (TfR) and ferritin, two proteins under posttranscriptional regulation of the IRP system. TfR protein levels increased more than twofold in cells depleted of Grx3, whereas the steady-state levels of ferritin were reduced to <10% of the control levels (Figure 4, A and B). In conclusion, Grx3 depletion caused an IRP1 activation resulting in the up-regulation of the iron importer and the down-regulation of the intracellular iron storage protein.

To determine the effects of these alterations on cellular iron levels, we measured the capacity of Grx3-depleted and scrambled siRNA–treated control HeLa cells to take up transferrin-bound ^{55}Fe. After 4 h of incubation, the ^{55}Fe level associated with the Grx3-depleted cells increased to 122 ± 4% of control cells (Figure 4E). This finding was consistent with the elevated IRE-binding activity of IRP1 and the increased levels of TfR. Moreover, Grx3 depletion led to a cellular redistribution of TfR and ferritin (Figure 5). Confocal immunofluorescence microscopy suggested the redistribution of TfR from the endosomal compartment to the plasma membrane and of ferritin from the cytosol to a compartment likely representing lysosomes, a step that is required for liberation of iron from ferritin (Asano *et al.* 2011). Together these facts argue against impaired iron acquisition as an explanation for the cytosolic Fe/S protein defects. The moderate increase in cellular iron was compatible with the hardly affected amounts and IRE-binding capacity of IRP2 (Figure 4, A, B, and D), which senses intracellular iron levels and is degraded under iron-replete conditions. Hence IRP2 levels have been suggested as an indirect measure for intracellular iron concentration (Rouault, 2006).
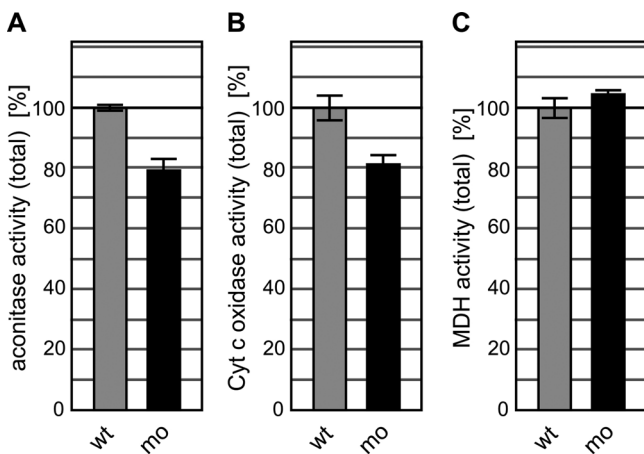
Grx3 depletion only mildly influences mitochondrial iron-dependent proteins

We finally analyzed the consequences of the depletion of human Grx3 on the activities of several mitochondrial iron-dependent enzymes. We used crude mitochondrial fractions (see Supplemental Figure S4) to determine the enzyme activities of aconitase, the heme-containing COX, and succinate dehydrogenase (respiratory complex II), which contains both heme and three Fe/S clusters. For the measurement of the activity of the Fe/S protein ferrochelatase, which catalyzes the last step of heme biosynthesis (Shepherd *et al.*, 2006), we used total HeLa cell extracts. On Grx3 depletion, the activities of COX, ferrochelatase, and succinate dehydrogenase were all decreased to ~80% of those of control cells treated with scrambled siRNA (Figure 6, A–C), although statistical significance of these decreases could not be demonstrated. Total mitochondrial aconitase activity did not change significantly (Figure 6D). Taken together, the results indicate that there was only weak influence of human Grx3 deficiency on mitochondrial iron proteins.

DISCUSSION

Our functional analysis of the cytosolic multidomain monothiol glutaredoxin Grx3 in both zebrafish and human cells provides strong evidence for a role of this protein in cellular iron metabolism.

FIGURE 3: Activities of total aconitase and cytochrome *c* oxidase are decreased in Grx3-depleted zebrafish embryos. Enzymatic activities of (A) aconitase, (B) cytochrome *c* oxidase, and (C) malate dehydrogenase (MDH) in pooled wild-type control (wt) and Grx3 morpholino-injected (mo) zebrafish embryos at 48 hpf. Because extracts of the entire embryos were analyzed, aconitase activity represents the sum of cytosolic and mitochondrial isoforms. MDH is an iron-independent control protein. All activities were normalized to the values of the respective wt samples. The 100% aconitase activity corresponds to 26.3 ± 0.4 mU/mg (of total protein), 100% cytochrome *c* oxidase activity to 136.4 ± 11.2 mU/mg, and 100% MDH activity to 0.98 ± 0.05 U/mg ($n = 3$–4).
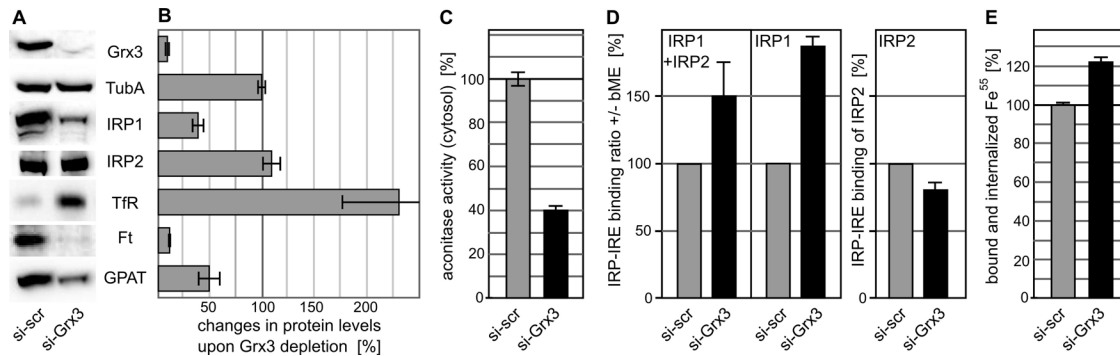
FIGURE 4: Grx3 depletion in HeLa cells impairs cytosolic iron-dependent processes despite an increased iron uptake. (A) Representative Western blots of control cells, transfected with scrambled siRNA (si-scr), and Grx3-depleted HeLa cells (si-Grx3) stained for Grx3, α-tubulin (TubA), IRP1 and IRP2, transferrin receptor, ferritin (Ft), and GPAT. (B) Densitometric quantification of Western blots as depicted in A from five independent experiments. (C) The enzyme activity of cytosolic aconitase was measured in the soluble fraction of a cell extract (see Supplemental Figure S4 for the efficiency of fractionation). Decrease in activity indicates impaired maturation of IRP1. Aconitase activity was normalized with respect to the control samples. The 100% activity corresponds to 47.8 ± 1.7 mU/mg of total cytosolic protein ($n = 5$). (D) Depletion of Grx3 impairs the IRE binding capacity of IRP1. Binding of both IRP1 and IRP2 to ^{32}P-labeled IRE of human ferritin mRNA was analyzed by RNA electrophoretic mobility shift assay. The IRE-binding capacity of IRP1 was measured after IRP2 supershift upon addition of IRP2 antiserum and calculated as the ratio of the respective binding activity without and with 1.7% (vol/vol) β-ME. Data were normalized to the respective ratio of control cells. The IRE-binding activity of IRP2 was measured after IRP1 supershift upon addition of IRP1 antiserum. The assay was performed in the presence of 0.3% (vol/vol) β-ME to increase the signal-to-noise ratio (Zumbrennen *et al.*, 2009), and results were normalized to the respective values of control cells. (E) Uptake of transferrin-bound ^{55}Fe into Grx3-depleted and scrambled siRNA-treated HeLa cells was allowed for 4 h and estimated by scintillation counting of crude cell extracts. The 100% values typically represent ~10,000 cpm.

Depletion of Grx3 was associated with defects in the biogenesis of both Fe/S proteins and heme and induced a prominent dysregulation of the cellular iron metabolism. In general, this phenotype closely resembles observations on the yeast homologues Grx3 and Grx4 (Mühlenhoff *et al.*, 2010). These cells showed strong impairment in the assembly of Fe/S proteins, heme, and iron-containing proteins, despite the fact that the cells accumulated iron in the cytosol. It was concluded from these studies that yeast Grx3/Grx4
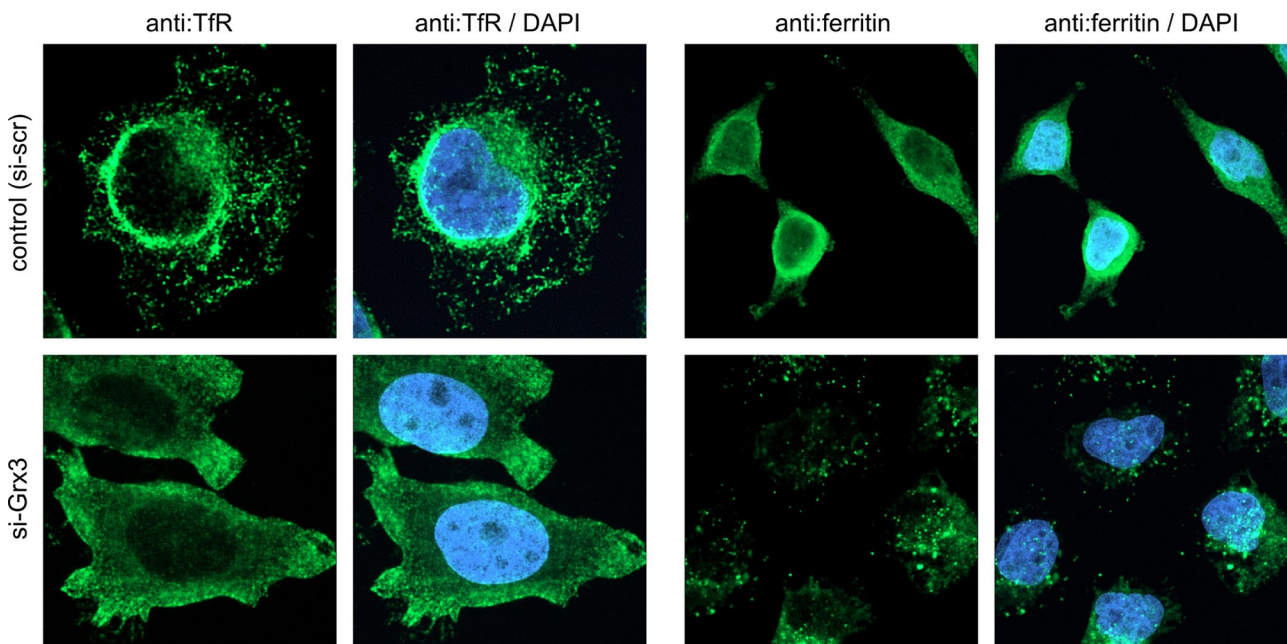

FIGURE 5: Grx3 depletion affects the subcellular distribution of the transferrin receptor and ferritin. HeLa cells transfected with scrambles control siRNA (si-scr) and Grx3 siRNA were fixated and stained for TfR (left) and ferritin (right) by immunofluorescence. Five layers in the volume ($z = 0.5$ μm) were scanned by confocal microscopy. For TfR, the focus was placed in close vicinity to the site of attachment of the cell to the glass slide, that is, on the cell membrane. For the analysis of ferritin distribution, the focus was placed ~1 μm ahead of the glass slide substrate within the cytosol.
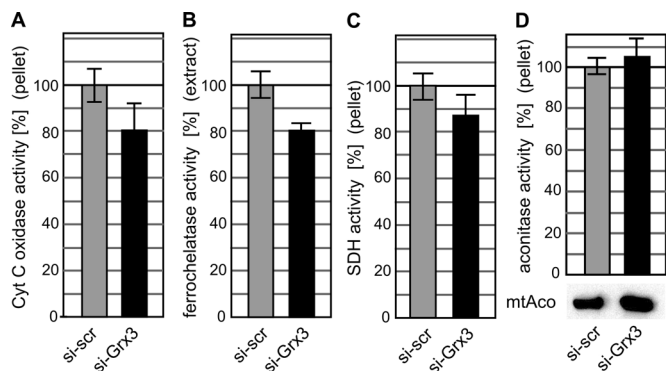
FIGURE 6: Grx3 depletion in HeLa cells only slightly affects the activities of mitochondrial iron-dependent enzymes. Activities of iron-dependent mitochondrial proteins in Grx3-depleted HeLa cells were measured in crude mitochondrial fractions or in total cell extracts (for ferrochelatase). (A) Cytochrome *c* oxidase activity, dependent on heme synthesis. (B) Ferrochelatase activity, Fe/S cluster dependent. (C) SDH activity, heme and Fe/S cluster dependent. (D) Mitochondrial aconitase, dependent on the insertion of a Fe/S cluster. For the efficiency of subcellular fractionation see Supplemental Figure S4. All activities were normalized to the scrambled siRNA-treated (si-scr) control samples. The 100% cytochrome *c* oxidase activity corresponds to 24.1 ± 2.1 mU/mg (of total mitochondrial protein), 100% SDH activity to 1.99 ± 0.14 U/mg, and 100% aconitase activity to 54.1 ± 3.5 mU/mg ($n = 3$–5).

perform a general function in intracellular iron trafficking and regulation. Despite the lack of functional complementation by ectopic expression of the human Grx3 gene in yeast (Hoffmann *et al.*, 2011), the present biochemical studies suggest that the function of this class of glutaredoxins in intracellular iron metabolism is conserved from yeast to human. The coordination of a bridging, glutathione-coordinated [2Fe-2S] cluster is essential for this task (Mühlenhoff *et al.*, 2010); however, the precise molecular mechanism of how these proteins function remains to be determined. One possibility is that they mobilize the iron from the cytosolic labile iron pool and thus facilitate the insertion of the metal ions into their target proteins. This scenario might require additional, target-specific metallochaperones for transfer and insertion of the iron. Only PCBP1 and PCBP2 of mammals have been identified as iron-specific chaperones for metal ion assembly into ferritin and the hypoxia-inducible factor prolyl hydroxylase (Shi *et al.*, 2008; Nandal *et al.*, 2011). Alternatively, Grx3 might operate at the metal insertion step by preparing the target proteins for accepting the iron ions. Additional biochemical studies will be needed to clarify the important mechanistic problem of glutaredoxin function.

Grx3-deficient yeast and human cells show a severe dysregulation of iron metabolism by turning on the iron acquisition pathways (Mühlenhoff *et al.*, 2010; this work). The molecular mechanisms of iron metabolism underlying this cellular situation differ radically in fungi and vertebrates. In the yeast *S. cerevisiae* a role of Grx3/Grx4 in iron regulation has long been demonstrated and can be separated from the proteins' role in intracellular iron trafficking (Ojeda *et al.*, 2006; Huynh *et al.*, 2009; Rutherford *et al.*, 2005). Grx3/Grx4 directly interact with the major iron-responding transcription factor Aft1 and modulate its activity. This function crucially involves the Grx-bound Fe/S cluster, which serves as a sensor of the intracellular iron status (Mühlenhoff *et al.*, 2010). Similarly, the iron metabolism in other fungi, such as *Schizosaccharomyces pombe*, is regulated by a direct interaction of Grx3 with iron-responsive transcription factors

(Jbel *et al.*, 2011; Vachon *et al.*, 2012; reviewed in Lill *et al.*, 2012; Philpott *et al.*, 2012). In contrast, the role of vertebrate Grx3 in iron regulation seems to be conferred indirectly via its iron-trafficking role during the assembly of the Fe/S cluster on IRP1. As shown here, defects in this process increase the IRE-interacting apo form of IRP1, leading to increased translation of the transferrin receptor and decreased ferritin translation. Concomitantly, the latter proteins were relocalized to the plasma membrane and lysosomes, respectively. Despite the radically different underlying mechanisms, the conserved monothiol Grxs act as key components of cellular iron regulation in eukaryotes.

The deficiency of cytosolic monothiol glutaredoxins also elicits defects in mitochondrial iron-dependent components (Mühlenhoff *et al.*, 2010; this work). However, in comparison to the severe effect on cytosolic and nuclear iron-dependent proteins, the defects in mitochondria appear to be only mild in yeast, zebrafish, and human Grx3-deficient cells. For instance, the Fe/S proteins aconitase and ferrochelatase or the respiratory complexes lost only 20% of their activities upon Grx3 depletion in zebrafish or human cells. From our experience, we expect no major metabolic effects from these small changes. In yeast the slightly stronger effects on mitochondrial iron-dependent proteins occur in a delayed manner compared with the cytosolic phenotype (Mühlenhoff *et al.*, 2010). We therefore cannot exclude that the mitochondrial defects are indirect side effects of the impairment of cytosolic iron-dependent processes. A notable exception is the hematopoietic system of zebrafish, which shows virtually no residual heme biosynthesis upon depletion of Grx3, demonstrating an essential function of cytosolic Grx3 in heme synthesis in erythroid cells, likely by helping to deliver iron to mitochondria (Mühlenhoff *et al.*, 2010). Conspicuously, the heme synthesis defect could not be reverted by simultaneous depletion of IRP1, that is, by removal of the translational inhibition of eALAS by apo-IRP1 binding to its IRE, demonstrated in Figure 2. Such an effect is observed for the depletion of the mitochondrial monothiol glutaredoxin Grx5, which is involved in the holo conversion of IRP1 to its aconitase form (Wingert *et al.*, 2005). This striking difference for the two glutaredoxins clearly indicates that Grx3 plays a crucial and general role in cytosolic iron metabolism that is not restricted to a regulatory function of iron-dependent processes via IRP1. Instead, cytosolic glutaredoxins play a conserved key role in delivering iron to iron-containing proteins. The function of Grx3 in cytosolic iron trafficking is also evident from the rescue of the heme biosynthesis defect in IRP1-deficient zebrafish by overproduction of Grx3. In the absence of IRP1-dependent iron regulation, low amounts of iron accumulate in the cells. A surplus of Grx3 may likely help to more efficiently distribute the residual iron to the iron-requiring processes.

Human Grx3 was first described as an interaction partner of protein kinase C-θ. In stimulated Jurkat cells (immortalized T-lymphocytes), Grx3 attenuated the activation of mitogen-activated c-Jun N-terminal kinase and, subsequently, the activation of the transcription factors AP-1 and Nf-κB (Witte *et al.*, 2000). Of note, a negative effect of iron deficiency on the response of T-cells toward mitogens has been discussed (Dallman, 1986). A potential connection between iron availability and signal transduction mediated by Grx3 may thus not be excluded. Grx3 was up-regulated in animal models of cardiac hypertrophy, and overexpression of Grx3 protected from cardiac hypertrophy (Jeong *et al.*, 2006; Cha *et al.*, 2008). Compared to Grx3^{+/+} littermates, heterozygous Grx3^{+/−} mice are more susceptible to the development of cardiac hypertrophy (Cha *et al.*, 2008). Decreased expression of the Fe/S cluster biogenesis protein frataxin in Friedreich's ataxia patients leads to mitochondrial iron overload and a decrease in the activities of Fe/S cluster–dependent

enzymes (Sheftel *et al.*, 2010; Ye and Rouault, 2010). In the majority of patients, these alterations lead to cardiomyopathy and cardiac hypertrophy (Rajagopalan *et al.*, 2010). How an impaired Grx3 function could be related to defects in Fe/S cluster assembly and how it contributes to cardiac hypertrophy via defects in cytosolic iron delivery remain to be determined. Grx3 is essential for embryonic development in mice, as homozygous Grx3$^{-/-}$ mice die between embryonic day (ED) 12.5 and 14.5 (Cha *et al.*, 2008). ED12.5 Grx3$^{-/-}$ embryos showed no obvious histological abnormalities when analyzed by hematoxylin/eosin staining; however, the embryos were of smaller body size and developed hemorrhages in the head. No detailed biochemical analysis of Grx3$^{-/-}$ embryos is available. Of note, E12.5 marks the onset of definitive erythropoiesis in the fetal liver (Steiner and Vogel, 1973; Brotherton *et al.*, 1979). These definitive erythrocytes quickly become the dominating cell type in the circulation, and their biogenesis is the major iron-consuming process of the embryos.

In summary, we demonstrate that the multidomain monothiol glutaredoxin Grx3 (PICOT) is an important component of intracellular iron homeostasis. Its deficiency affects numerous iron-containing proteins and impairs both Fe/S protein and heme biosynthesis, even though the Grx3-deficient cell is iron replete. These results and our previous work on yeast Grx3/Grx4 provide strong evidence for a conserved role of this class of glutaredoxins in the iron metabolism of eukaryotic cells.

MATERIALS AND METHODS

Zebrafish
Zebrafish were kept and raised in standard conditions; embryos were staged according to Kimmel *et al.* (1995). Whole-mount in situ hybridization was performed according to standard protocols. Embryos were mounted in low-melting agarose or glycerol and analyzed with a Leica MZ16 stereomicroscope (Leica, Wetzlar, Germany) equipped with a Leica DFC300FX camera.

The morpholino oligomers (Grx3, 5′-ATGCCGCGTCCGT-GAAGTTCGCCAT-3′; IRP1, Wingert *et al.*, 2005) were obtained from Gene Tools (Philomath, OR) and dissolved to a concentration of 3 mM in distilled H$_2$O. A 1.5-nl amount of a 1/40 (Grx3) or 1/80 (IRP1) dilution was injected into single-cell eggs using a Femtojet microinjector (Eppendorf, Hauppauge, NY). Capped mRNA was transcribed from the zfGrx3 open reading frame cloned into pCS2 using the mMessage/mMachine Kit (Ambion, Austin, TX) according to the manufacturer's instructions.

For measurement of enzymatic activities, whole zebrafish embryos (48 hpf) were resuspended in TNETG buffer (20 mM Tris-HCl, pH 7.4, 50 mM NaCl, 2.5 mM EDTA, 10% glycerol, 0.5% Triton X-100), lysed by vortexing with glass beads (0.5 volume glass beads per volume buffer), and cleared by centrifugation.

Hemoglobin staining of zebrafish embryos
For *o*-dianisidine staining, dechorionized embryos were incubated in 0.6 mg/ml *o*-dianisidine, 10 mM sodium acetate, pH 4.5, 0.65% hydrogen peroxide, and 40% ethanol for 15 min, followed by several washing steps in phosphate-buffered saline (PBS). Embryos were fixated in 4% paraformaldehyde and analyzed by light microscopy. For DAF staining of embryos a stock solution of 10 mg/ml DAF (D17106; Sigma-Aldrich, St. Louis, MO) in 90% acetic acid was prepared. Dechorionized embryos were incubated with 0.1 mg/ml DAF in 200 mM Tris-HCl, pH 7.0, for 30 min. Next hydrogen peroxide was added to a final concentration of 0.3%, and the samples were incubated for another 20 min. After several washing steps with PBS, the embryos were analyzed by bright-field microscopy.

Cell culture
HeLa cells were cultivated at 37°C in a 90% humidified atmosphere containing 5% CO$_2$ and grown in low-glucose DMEM (PAA, Pasching, Austria) supplemented with 10% heat-inactivated fetal calf serum (FCS), 100 U/ml penicillin, and 100 U/ml streptomycin.

Cells were transfected with siRNA (Eurogentec, Seraing, Belgium) against Grx3 (sense, GCC UAU UCC AGU UGG CCU Att; antisense, UAG GCC AAC UGG AAU AGG Ctt) and unspecific "scrambled" siRNA as control (sense, CAU UCA CUC AGG UCA UCA Att; antisense, CUG AUG ACC UGA GUG AAU Att). Further siRNAs were evaluated to confirm the specificity of the siRNA approach (Supplemental Figure S3). HeLa cells, 3.5 million, were electroporated with 15 μg of siRNA in 600 μl of electroporation buffer (21 mM 4-(2-hydroxyethyl)-1-piperazineethanesulfonic acid [HEPES], pH 7.15, 137 mM NaCl, 5 mM KCl, 0.7 mM Na$_2$HPO$_4$, 6 mM D-glucose) at 250 V and 1500 μF (modified from Lillig *et al.*, 2005, and Stehling *et al.*, 2007). Fresh FCS was added to the cells before seeding them in conditioned medium containing 80% fresh medium. Cells were transfected a second time after 3 d and harvested 3 d later, that is, at day 6 after the first transfection. Knockdown of Grx3 was verified by immunoblotting and quantitative PCR (primer pair, 5′-GAT GAA GAA GTT CGG CAA GG-3′ and 5′-GGC AGC AAT TCA CCA TTT TC-3′) using the absolute qPCR SYBR-Green Mix Plus Kit as recommended by the manufacturer (Thermo Scientific, Waltham, MA).

Iron uptake was assayed by incubation of HeLa cells with transferrin-bound ^{55}Fe for 4 h, followed by several washing steps with PBS, until essentially no residual radioactivity could be detected in the supernatant. The ^{55}Fe bound to and taken up by the cells was quantified by scintillation counting. Transferrin-^{55}Fe was prepared by dropwise addition of 24 μl of sodium citrate (1.7 M) to 13 μl of ^{55}Fe solution containing 23 μg of iron in 0.5 M HCl, followed by addition of 16 mg of transferrin (Sigma-Aldrich) diluted in 300 μl of sodium hydrogen carbonate (1 M) and 165 μl of PBS.

For analysis by immunofluorescence, HeLa cells were seeded onto glass slides, fixated with 4% paraformaldehyde for 20 min at room temperature, washed with PBS, permeabilized in 10 mM HEPES, 2% BSA, and 0.3% Triton X-100 in PBS for 1 h, and incubated with the primary antibody overnight at 4°C. Alexa 488–labeled secondary antibodies (Invitrogen, Carlsbad, CA) were used for detection, and 4′,6-diamidino-2-phenylindole (Sigma-Aldrich) was used for staining of the nuclei. Slides were mounted with Mowiol and analyzed with a Leica LCS SP5 microscope equipped with a 63× oil immersion objective with a numerical aperture of 1.4. Scans were analyzed with the Huygens software package (Scientific Volume Imaging, Hilversum, Netherlands).

Enzymatic activity assays
Cell fractionation, colorimetric activity measurements of iron-dependent enzymes, RNA electrophoretic mobility shift assays, and immunoblot analysis were performed as outlined in Biederbick *et al.* (2006), Stehling *et al.* (2007, 2009), and Godoy *et al.* (2011). The zebrafish-specific ALAS2 antibody was a test sample from GeneTex (Irvine CA; ZF127887, dilution 1:500). Intensities of immunoblot signals were quantified using ImageJ (National Institutes of Health, Bethesda, MD). For the determination of ferrochelatase activity, frozen cell pellets were resuspended in mitobuffer (20 mM HEPES, pH 7.4, 50 mM KCl, 1 mM MgSO$_4$, 0.6 M sorbitol). We incubated 200 μg of protein, 1 mM ascorbate, 2 mM succinate, 2.5 μM deuteroporphyrin, and 1 μCi/10 μl ^{55}FeCl$_2$ for 15 min at 30°C gentle shaking. Subsequently, samples were put on ice, stop-solution (100 mM FeCl$_3$ in 5 M HCl) was added, and heme was extracted by

butyl acetate. Samples were vortexed twice for 30 s and centrifuged for 5 min at 14,000 rpm, and the radioactivity extracted to the organic phase was quantified by scintillation counting.

ACKNOWLEDGMENTS

REFERENCES

Asano T, Komatsu M, Yamaguchi-Iwai Y, Ishikawa F, Mizushima N, Iwai K (2011). Distinct mechanisms of ferritin delivery to lysosomes in iron-depleted and iron-replete cells. Mol Cell Biol 31, 2040–2052.

Biederbick A, Stehling O, Rösser R, Niggemeyer B, Nakai Y, Elsässer H-P, Lill R (2006). Role of human mitochondrial Nfs1 in cytosolic iron-sulfur protein biogenesis and iron regulation. Mol Cell Biol 26, 5675–5687.

Brotherton TW, Chui DH, Gauldie J, Patterson M (1979). Hemoglobin ontogeny during normal mouse fetal development. Proc Natl Acad Sci USA 76, 2853–2857.

Brynczka C, Labhart P, Merrick BA (2007). NGF-mediated transcriptional targets of p53 in PC12 neuronal differentiation. BMC Genomics 8, 139.

Cairo G, Bernuzzi F, Recalcati S (2006). A precious metal: iron, an essential nutrient for all cells. Genes Nutr 1, 25–39.

Camaschella C, Campanella A, De Falco L, Boschetto L, Merlini R, Silvestri L, Levi S, Iolascon A (2007). The human counterpart of zebrafish shiraz shows sideroblastic-like microcytic anemia and iron overload. Blood 110, 1353–1358.

Cha H et al. (2008). PICOT is a critical regulator of cardiac hypertrophy and cardiomyocyte contractility. J Mol Cell Cardiol 45, 796–803.

Dallman PR (1986). Biochemical basis for the manifestations of iron deficiency. Annu Rev Nutr 6, 13–40.

Feng Y, Zhong N, Rouhier N, Hase T, Kusunoki M, Jacquot J-P, Jin C, Xia B (2006). Structural insight into poplar glutaredoxin C1 with a bridging iron-sulfur cluster at the active site. Biochemistry 45, 7998–8008.

Godoy JR, Funke M, Ackermann W, Haunhorst P, Oesteritz S, Capani F, Elsässer HP, Lillig CH (2011). Redox atlas of the mouse: immunohistochemical detection of glutaredoxin-, peroxiredoxin-, and thioredoxin-family proteins in various tissues of the laboratory mouse. Biochim Biophys Acta 1810, 2–92.

Guo B, Phillips JD, Yu Y, Leibold EA (1995). Iron regulates the intracellular degradation of iron regulatory protein 2 by the proteasome. J Biol Chem 270, 21645–21651.

Hentze MW, Muckenthaler MU, Galy B, Camaschella C (2010). Two to tango: regulation of Mammalian iron homeostasis. Cell 142, 24–38.

Herrero E, de la Torre-Ruiz MA (2007). Monothiol glutaredoxins: a common domain for multiple functions. Cell Mol Life Sci 64, 1518–1530.

Hoffmann B, Uzarska MA, Berndt C, Godoy JR, Haunhorst P, Lill R, Lillig CH, Muhlenhoff U (2011). The multi-domain thioredoxin-monothiol glutaredoxins represent a distinct functional group. Antioxid Redox Signal 15, 19–30.

Huynh BH, Johnson MK, Outten CE, Li H, Mapolelo DT, Dingra NN, Naik SG, Lees NS, Hoffman BM, Riggs-Gelasco PJ (2009). The yeast iron regulatory proteins Grx3/4 and Fra2 form heterodimeric complexes containing a [2Fe-2S] cluster with cysteinyl and histidyl ligation. Biochemistry 48, 9569–9581.

Jbel M, Mercier A, Labbé S (2011). Grx4 monothiol glutaredoxin is required for iron limitation-dependent inhibition of Fep1. Eukaryot Cell 10, 629–645.

Jeong D et al. (2006). PICOT inhibits cardiac hypertrophy and enhances ventricular function and cardiomyocyte contractility. Circ Res 99, 307–314.

Jeong D, Kim JM, Cha H, Oh JG, Park J, Yun S-H, Ju E-S, Jeon E-S, Hajjar RJ, Park WJ (2008). PICOT attenuates cardiac hypertrophy by disrupting calcineurin-NFAT signaling. Circ Res 102, 711–719.

Kimmel CB, Ballard WW, Kimmel SR, Ullmann B, Schilling TF (1995). Stages of embryonic development of the zebrafish. Dev Dyn 203, 253–310.

Li H, Ginzburg YZ (2010). Crosstalk between iron metabolism and erythropoiesis. Adv Hematol 2010, 605435.

Lill R, Hoffmann B, Molik S, Pierik AJ, Rietzschel N, Stehling O, Uzarska MA, Webert H, Wilbrecht C, Mühlenhoff U (2012). The role of mitochondria in cellular iron-sulfur protein biogenesis and iron metabolism. Biochim Biophys Acta 1823, 1491–1508.

Lillig CH, Berndt C, Holmgren A (2008). Glutaredoxin systems. Biochim Biophys Acta 1780, 1304–1317.

Lillig CH, Berndt C, Vergnolle O, Lönn ME, Hudemann C, Bill E, Holmgren A (2005). Characterization of human glutaredoxin 2 as iron-sulfur protein: a possible role as redox sensor. Proc Natl Acad Sci USA 102, 8168–8173.

Muckenthaler MU, Galy B, Hentze MW (2008). Systemic iron homeostasis and the iron-responsive element/iron-regulatory protein (IRE/IRP) regulatory network. Annu Rev Nutr 28, 197–213.

Mühlenhoff U, Gerber J, Richhardt N, Lill R (2003). Components involved in assembly and dislocation of iron-sulfur clusters on the scaffold protein Isu1p. EMBO J 22, 4815–4825.

Mühlenhoff U et al. (2010). Cytosolic monothiol glutaredoxins function in intracellular iron sensing and trafficking via their bound iron-sulfur cluster. Cell Metab 12, 373–385.

Nandal A, Ruiz JC, Subramanian P, Ghimire-Rijal S, Sinnamon RA, Stemmler TL, Bruick RK, Philpott CC (2011). Activation of the HIF prolyl hydroxylase by the iron chaperones PCBP1 and PCBP2. Cell Metab 14, 647–657.

Ojeda L, Keller G, Muhlenhoff U, Rutherford JC, Lill R, Winge DR (2006). Role of glutaredoxin-3 and glutaredoxin-4 in the iron regulation of the Aft1 transcriptional activator in Saccharomyces cerevisiae. J Biol Chem 281, 17661–17669.

Philpott CC, Leidgens S, Frey AG (2012). Metabolic remodeling in iron-deficient fungi. Biochim Biophys Acta 1823, 1509–1520.

Picciocchi A, Saguez C, Boussac A, Cassier-Chauvat C, Chauvat F (2007). CGFS-type monothiol glutaredoxins from the cyanobacterium Synechocystis PCC6803 and other evolutionary distant model organisms possess a glutathione-ligated [2Fe-2S] cluster. Biochemistry 46, 15018–15026.

Rajagopalan B, Francis JM, Cooke F, Korlipara LVP, Blamire AM, Schapira AHV, Madan J, Neubauer S, Cooper JM (2010). Analysis of the factors influencing the cardiac phenotype in Friedreich's ataxia. Mov Disord 25, 846–852.

Richardson DR, Ponka P (1997). The molecular mechanisms of the metabolism and transport of iron in normal and neoplastic cells. Biochim Biophys Acta 1331, 1–40.

Rodríguez-Manzaneque MT, Ros J, Cabiscol E, Sorribas A, Herrero E (1999). Grx5 glutaredoxin plays a central role in protection against protein oxidative damage in Saccharomyces cerevisiae. Mol Cell Biol 19, 8180–8190.

Rodríguez-Manzaneque MT, Tamarit J, Bellí G, Ros J, Herrero E (2002). Grx5 is a mitochondrial glutaredoxin required for the activity of iron/sulfur enzymes. Mol Biol Cell 13, 1109–1121.

Rouault TA (2006). The role of iron regulatory proteins in mammalian iron homeostasis and disease. Nat Chem Biol 2, 406–414.

Rutherford JC, Ojeda L, Balk J, Mühlenhoff U, Lill R, Winge DR (2005). Activation of the iron regulon by the yeast Aft1/Aft2 transcription factors depends on mitochondrial but not cytosolic iron-sulfur protein biogenesis. J Biol Chem 280, 10135–10140.

Salahudeen AA, Thompson JW, Ruiz JC, Ma H-W, Kinch LN, Li Q, Grishin NV, Bruick RK (2009). An E3 ligase possessing an iron-responsive hemerythrin domain is a regulator of iron homeostasis. Science 326, 722–726.

Schranzhofer M, Schifrer M, Cabrera JA, Kopp S, Chiba P, Beug H, Müllner EW (2006). Remodeling the regulation of iron metabolism during erythroid differentiation to ensure efficient heme biosynthesis. Blood 107, 4159–4167.

Sheftel A, Stehling O, Lill R (2010). Iron-sulfur proteins in health and disease. Trends Endocrinol Metab 21, 302–314.

Shepherd M, Dailey TA, Dailey HA (2006). A new class of [2Fe-2S]-cluster-containing protoporphyrin (IX) ferrochelatases. Biochem J 397, 47–52.

Shi H, Bencze KZ, Stemmler TL, Philpott CC (2008). A cytosolic iron chaperone that delivers iron to ferritin. Science 320, 1207–1210.

Stehling O, Netz DJA, Niggemeyer B, Rösser R, Eisenstein RS, Puccio H, Pierik AJ, Lill R (2008). Human Nbp35 is essential for both cytosolic iron-sulfur protein assembly and iron homeostasis. Mol Cell Biol 28, 5517–5528.

Stehling O, Sheftel AD, Lill R (2009). Controlled expression of iron-sulfur cluster assembly components for respiratory chain complexes in mammalian cells. Methods Enzymol 456, 209–231.

Stehling O, Smith PM, Biederbick A, Balk J, Lill R, Mühlenhoff U (2007). Investigation of iron-sulfur protein maturation in eukaryotes. Methods Mol Biol 372, 325–342.

Steiner R, Vogel H (1973). On the kinetics of erythroid cell differentiation in fetal mice. I. Microspectrophotometric determination of the hemoglobin content in erythroid cells during gestation. J Cell Physiol 81, 323–338.

Vachon P, Mercier A, Jbel M, Labbé S (2012). The monothiol glutaredoxin grx4 exerts an iron-dependent inhibitory effect on php4 function. Eukaryotic Cell 11, 806–819.

Vashisht AA et al. (2009). Control of iron homeostasis by an iron-regulated ubiquitin ligase. Science 326, 718–721.

Wingert RA et al. (2005). Deficiency of glutaredoxin 5 reveals Fe-S clusters are required for vertebrate haem synthesis. Nature 436, 1035–1039.

Witte S, Villalba M, Bi K, Liu Y, Isakov N, Altman A (2000). Inhibition of the c-Jun N-terminal kinase/AP-1 and NF-kappaB pathways by PICOT, a novel protein kinase C-interacting protein with a thioredoxin homology domain. J Biol Chem 275, 1902–1909.

Ye H, Rouault TA (2010). Human iron-sulfur cluster assembly, cellular iron homeostasis, and disease. Biochemistry 49, 4945–4956.

Zhou G, Broyles SS, Dixon JE, Zalkin H (1992). Avian glutamine phosphoribosylpyrophosphate amidotransferase propeptide processing and activity are dependent upon essential cysteine residues. J Biol Chem 267, 7936–7942.

Zumbrennen KB, Wallander ML, Romney SJ, Leibold EA (2009). Cysteine oxidation regulates the RNA-binding activity of iron regulatory protein 2. Mol Cell Biol 29, 2219–2229.